CHAPTER 5

DEVELOPMENT OF THE PREDICTIVE MODEL

5.1. Introduction

All considered parameters influencing the stability of the dump slope structures play a significant role. They also contribute differently due to their interplay in a cumulative way. Hence, a statistical model has been obtained for the cumulative effect of these parameters. The behaviour of the maximum Horizontal Displacement (XDIS) and Shear Strain Increment (SSI) related to FoS are also evaluated. In addition, criteria for stability state classification and the corresponding extent of the affected zone are also discussed. The reduction factor of the performance measuring parameters due to the presence of a water table is derived here.

5.2. Statistical Model

Equation 5.1 represents the relationship of the total dump height (T), bench height (H), bench slope angle (A), bench width (W), density (ρ), cohesion (C), and friction angle (φ) with the factor of safety (FoS). The model had an R^2 value of 0.98 and an F-value of 2772 with a standard error of 0.047. The overall P-value of the model was zero. Table 5.1 summarizes that the P-values associated with independent parameters were also zero. Thus, the statistical performance indicator implies that predicted values were very close to the actual value of the dependent variable, and the same is also reflected in Figure 5.1. The regression coefficients show that bench slope angle and friction angle were the most influencing parameters whereas density and total dump height were the least affecting parameters (Table 5.1). Equation 5.1 was obtained for a specific range of independent parameters (Table 5.2). In FoS calculation, the friction angle was taken with tangent function, and the bench slope angle with cosine as well as sine function as described in

LEM (Abramson et al. 2002). The bench slope angle was considered with the sine function as it provided less error in prediction.

$$FoS = 41.28\frac{X^{0.79}C^{0.24}W^{0.28}}{T^{0.17}H^{0.33}Y^{1.06}\rho^{0.21}} \quad (5.1)$$

T: total dump height (meter), H: bench height (meter), Y: sin(A), A: bench slope angle (°), W: bench width (meter), ρ: density (kg/m^3), C: cohesion (MPa), X: tan(φ), φ: friction angle (°)

Table 5.1 Coefficients and P-value of independent parameters

Parameters	Coefficients	P-value
Intercept	3.72	5.1E-102
T	-0.17	6.8E-86
H	-0.33	1.3E-129
A	-1.06	1.9E-89
W	0.28	2.5E-121
C	0.24	1.1E-201
φ	0.79	6.3E-206
ρ	-0.21	1.4E-32

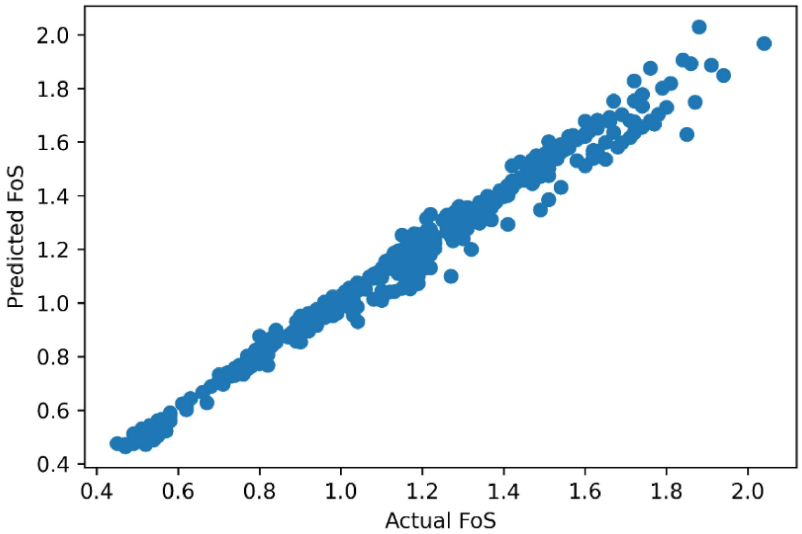

Fig. 5.1 Actual versus Predicted factor of safety

Table 5.2 Range of independent parameters incorporated in the statistical model

Parameters	**Range**
Total Dump Height (m)	20 - 420
Bench Height (m)	10 - 50
Slope Angle (°)	30 - 50
Bench Width (m)	5 - 40
Cohesion (MPa)	0.01 – 0.09
Friction Angle (°)	16 - 40
Density (kg/m^3)	1300 - 2300

5.3. Sensitivity Analysis of Output Parameters

The max horizontal displacement and shear strain increment have the ability to indicate the instability prone zone and failed part in large-size multi-bench dump slope structure compared to the safety factor. The parametric study showed that the change in magnitude of XDIS and SSI was significant compared to the safety factor. Therefore, the sensitivity of the numerical modelling based generated output parameters, i.e., XDIS and SSI related to FoS are discussed here. Figure 5.2 illustrates the occurrence of XDIS corresponding to the FoS of this study. Similarly, Figure 5.3 describes the variation in the magnitude of SSI against FoS. It was examined that the extent of material flow in the horizontal direction and strain generation increased drastically when the stability state condition changed from stable to unstable state. The XDIS and SSI followed the same trend as depicted in Figures 5.2 (a) and 5.3 (a), respectively, but behaviour changed when FoS was greater than one (Figures 5.2 (b) and 5.3 (b)). It was concluded that XDIS was less than 10 mm in most cases when FoS was greater than 1.30. The XDIS mainly varied

between 10 to 100 mm for FoS of 1 to 1.30. In Figure 5.3 (b), the majority of the cases possessed SSI below 0.0025 when FoS > 1.30 and varied between 0.0025 to 0.03 for the FoS range of 1 to 1.30.

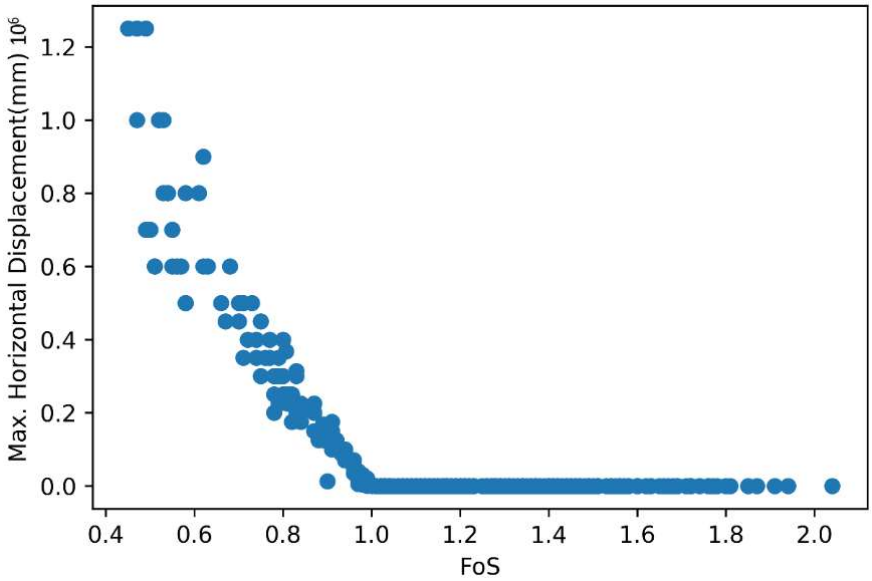

(a) FoS range based on 386 cases

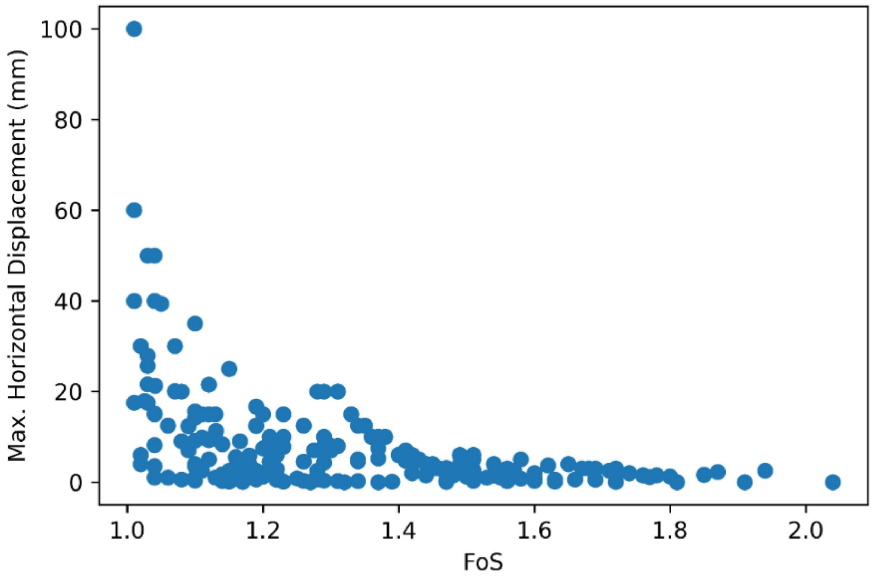

(b) FoS >1.0

Fig. 5.2 Factor of Safety versus Max Horizontal Displacement

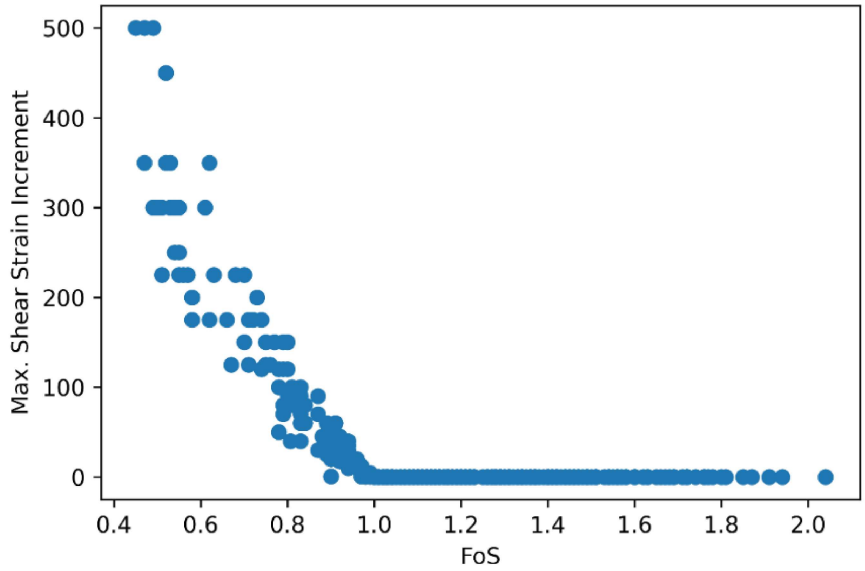

(a) FoS range based on 386 cases

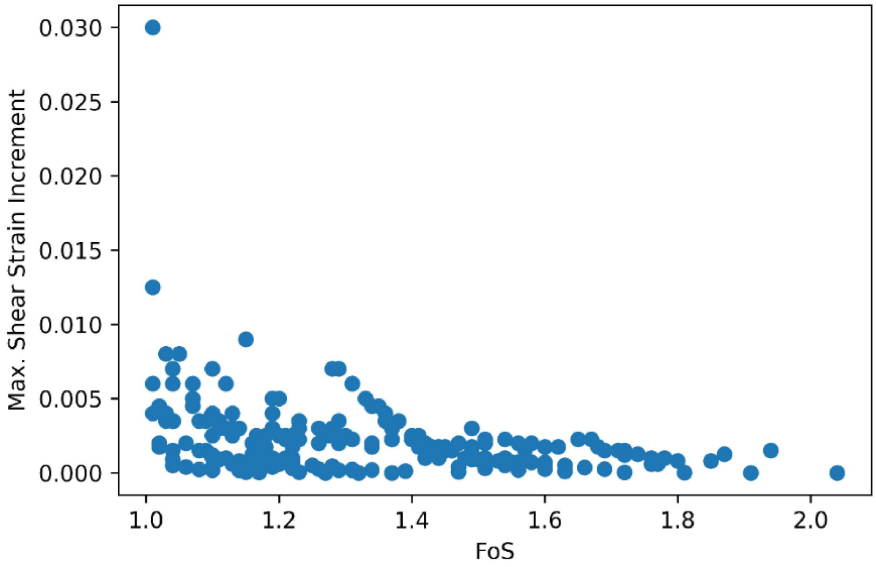

(b)FoS >1.0

Fig. 5.3 Factor of Safety versus Max Shear Strain Increment

5.4. Stability State Classification and Mapping of Instability Prone Zone

The dump structure would be stable if the maximum horizontal displacement is less than 10 mm. The design limit of the maximum displacement for a stable dump slope was decided on the basis of engineering judgment and field experience, which was later

confirmed by Slope Stability Radar (SSR) measurements (IIT-BHU 2019a). The same was also confirmed from the conclusion of Figure 5.2 (b) that XDIS and SSI did not change significantly during a marginal change in the stable state FoS range (FoS>1.30). However, in a critically stable state, XDIS and SSI changed significantly when a marginal change occurred in the critically stable state FoS range (1<FoS≤1.30). Hence, this fact was utilized to define the critically stable state by classifying the range of FoS, XDIS, and SSI.

The dump slope was in an unstable state when FoS was less than one. The cases where FoS was greater than one were subdivided into the stable and critically stable states, as represented in Figure 5.4. The dump slope structure had a max horizontal displacement of less than 10 mm with FoS greater than one and was classified as stable. In the critically stable state, FoS was greater than one with XDIS greater than 10 mm. All 386 simulated models were passed through the stability state classification algorithm. The results are summarized in Table 5.3. The stable state indicated that FoS > 1.30, XDIS < 10 mm with SSI < 0.0025. The critically stable state covered the range of FoS from 1 – 1.30, XDIS from 10 – 100 mm, and SSI from 0.0025 – 0.03. In an unstable state, the FoS was less than one, and XDIS and SSI were greater than 100 mm and 0.03, respectively. About 5% of exceptional stable cases possessed XDIS less than 10 mm and SSI almost nearly at the boundary point of stable and critically stable state (0.0025), but FoS was between 1 to 1.30. In these cases, the total dump height and bench slope angle were low. The bench width was less than the bench height. The density and shear strength were present in the moderate range. Approx 0.52% of critically stable cases depicted XDIS greater than 10 mm with variation in SSI between 0.0025 to 0.03 but had FoS greater than 1.30. In these cases, the total dump height, density, and cohesion were high.

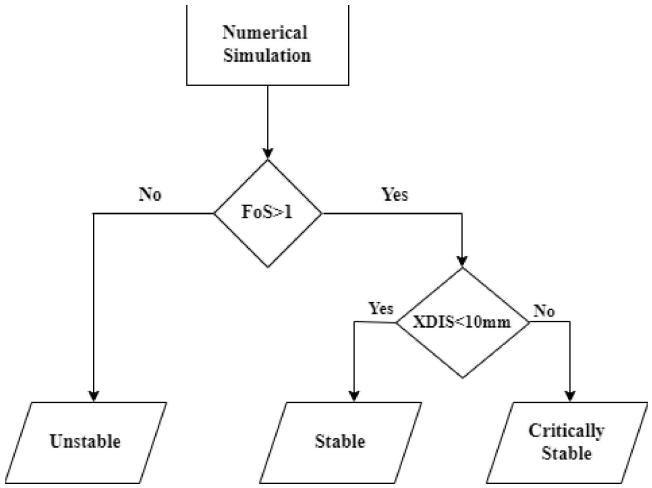

Fig. 5.4 Stability state classification of dump slope structure

Table 5.3 Classification of dump slope stability assessment parameters based on stability states

Stability State	FoS	XDIS (mm)	SSI
Stable	>1.30	<10	<0.0025
Critically Stable	1-1.30	10 – 100	0.0025 – 0.03
Unstable	<1	>100	>0.03

Three cases related to the stable, critically stable, and unstable states were selected from the solved models. The affected parts of the dump slopes corresponding to the different stability states have been illustrated in Figures 5.5 to 5.7. The input and output parameters of the stable, critically stable, and unstable cases are summarized in Table 5.4. Figure 5.5 depicts the stable state of the dump slope structure. The total dump height was 180 m, bench height was 30 m, bench slope angle was 40°, bench width was 30 m, cohesion was 0.05 MPa, and friction angle was 28° with a density of 1300 kg/m^3. The stable state of the dump slope structure transformed into a critically stable state upon reduction of the bench width from 30 to 15 m and increasing the OB density from 1300 to 1800 kg/m^3 with no change in the remaining geometrical and shear strength parameters (Figure 5.6).

The dump slope structure failed upon reducing the cohesion of the stable state from 0.05 to 0.01 MPa and increasing the OB density from 1300 to 1800 kg/m^3 without alteration of the rest of the stability governing parameters (Figure 5.7). The FoS, XDIS, and SSI of these cases agreed with Table 5.3.

Table 5.4 Stability governing and output parameters of different stability states

	Stable State	**Critically Stable State**	**Unstable State**
Total Dump Height (m)	180	180	180
Bench Height (m)	30	30	30
Slope Angle (°)	40	40	40
Bench Width (m)	30	15	30
Cohesion (MPa)	0.05	0.05	0.01
Friction Angle (°)	28	28	28
Density (kg/m^3)	1300	1800	1800
FoS	1.49	1.12	0.92
XDIS (mm)	3	15	125000
SSI	0.00125	0.003	17.5

The dump slope structure area that experienced horizontal displacement greater than 10 mm is illustrated in black. The shear strain increment indicated the instability initialization portion in the dump slope structure. In the stable state, XDIS was less than 10 mm. Therefore, black-coloured zones were absent, as illustrated in Figure 5.5 (a). The SSI was concentrated at the toe of the 2nd and 3rd bench from the bottom but it was within the stable state condition limit (Figure 5.5 (b)).

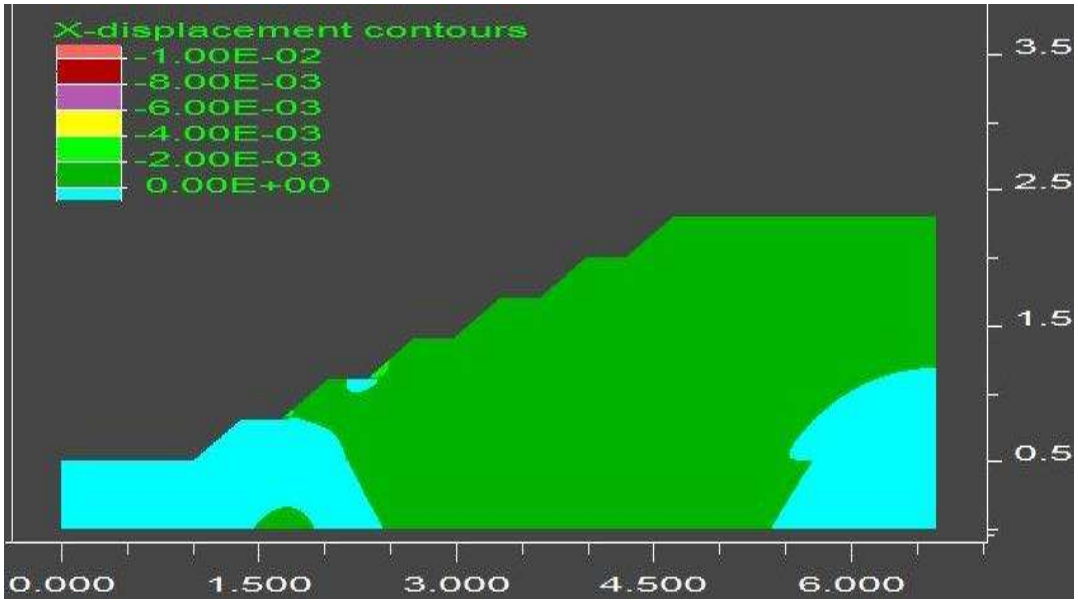

(a)

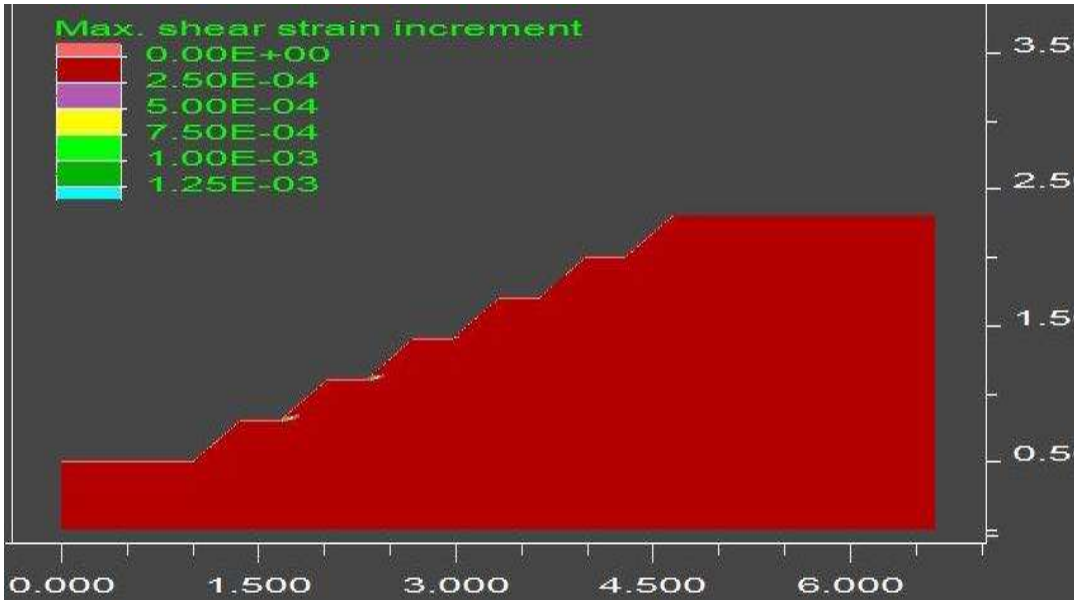

(b)

Fig. 5.5 Horizontal displacement (a) and shear strain (b) plot of stable dump slope structure (1 unit of X & Y axis = 100m)

In a critically stable state condition, three benches from the bottom experienced XDIS greater than 10 mm (Figure 5.6 (a)). The XDIS was concentrated at the toe of the bottom three benches. It also expanded along and away from the slope surface in the 2nd and 3rd bottom most benches. The extent of max XDIS decreased in the 3rd bench compared to the 2nd bench and was negligible in the toe of the 4th bench. The shear strain increment

was also observed in four benches from the bottom (Figure 5.6 (b)). It showed that failure initiation started from the toe of the bench. The magnitude of SSI was high in 2nd bench compared to the remaining three benches. The extent of SSI was more significant in the bottommost bench and reduced gradually towards the upper benches.

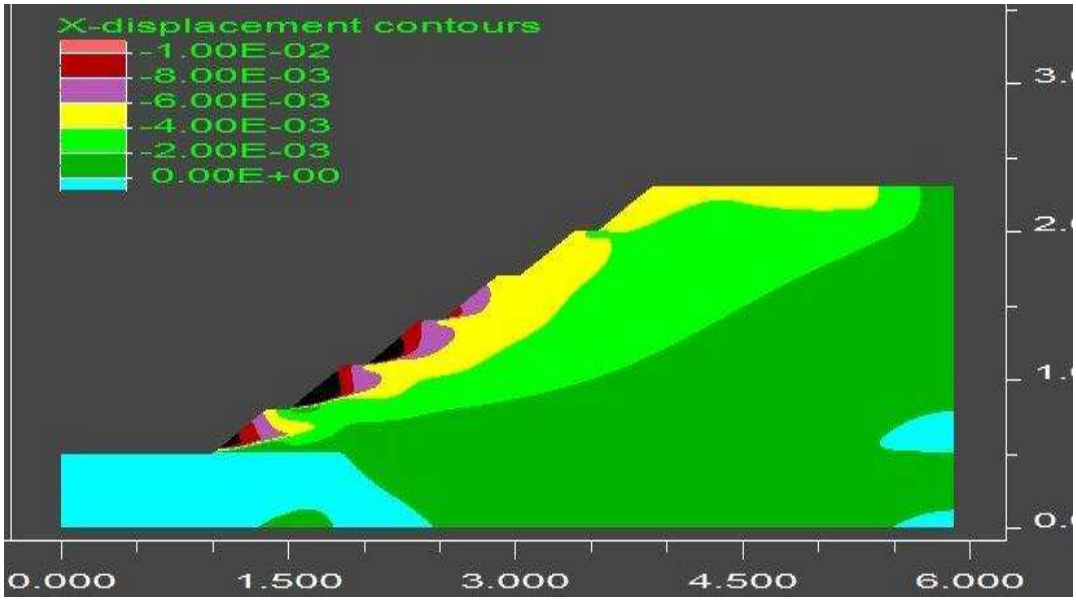

(a)

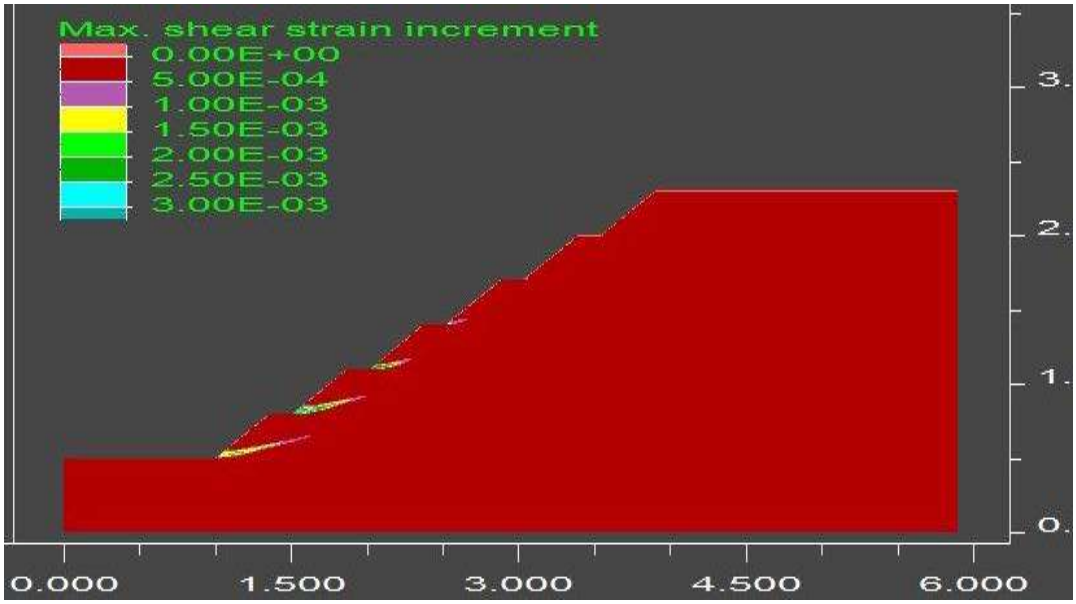

(b)

Fig. 5.6 Horizontal displacement (a) and shear strain (b) plot of critically stable dump slope structure (1 unit of X & Y axis = 100m)

In an unstable state, the scenario of XDIS and SSI changed drastically, as shown in Figure 5.7. All benches from bottom to top encountered XDIS greater than 10 mm and collapsed (Figure 5.7 (a)). The affected area was approximately the same in all benches except the topmost bench. In the topmost bench, the influenced zone extended further from the crest compared to the rest of the benches. The same catastrophic failure was also confirmed from the SSI plot (Figure 5.7 (b)). The SSI propagated from toe to beyond the crest in all the benches. The circular slip surface was formed in all benches with a minor difference in SSI magnitude.

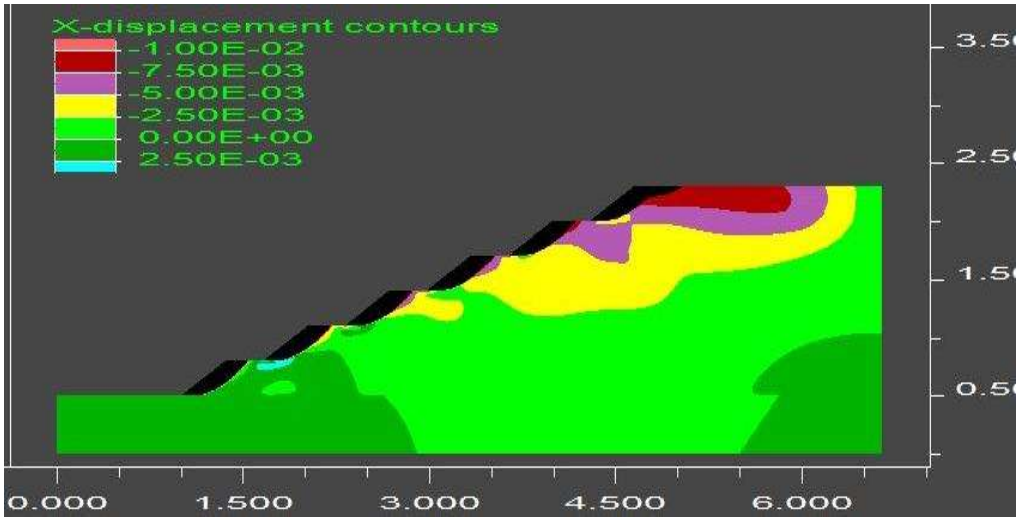

(a)

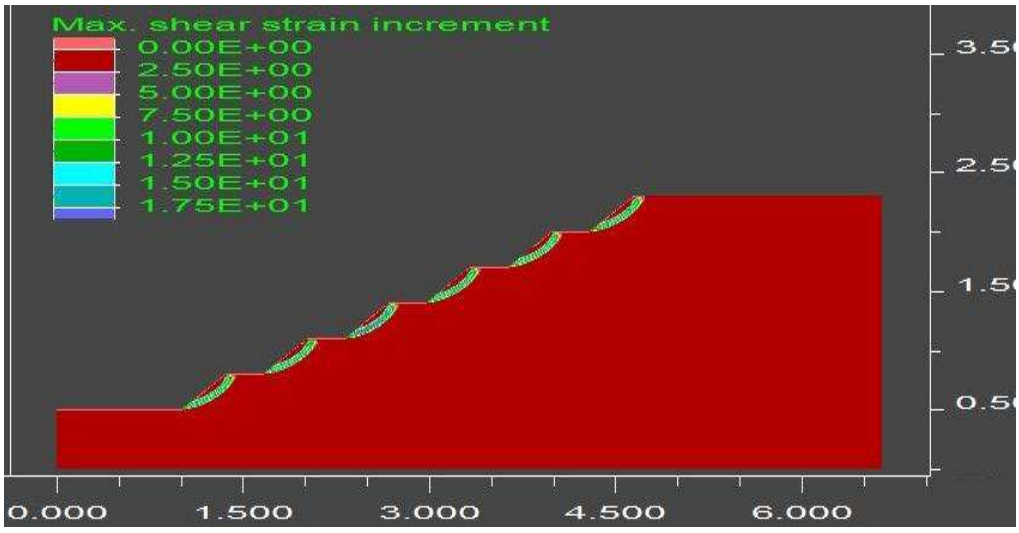

(b)

Fig. 5.7 Horizontal displacement (a) and shear strain (b) plot of unstable dump slope structure (1 unit of X & Y axis = 100m)

5.5. Study of the Effect of Water Table

The water table sensitivity analysis determined the FoS, XDIS, and SSI at different water tables for the various dump heights. The severity of the impact of the water table was identified by determining the ratio of the FoS, XDIS, and SSI in the presence of the water table to FoS, XDIS, and SSI in the absence of the water table, respectively (Equations 5.2 – 5.4). FoSR (FoS ratio), XDISR (XDIS ratio) and SSIR (SSI ratio) were the water table impact factors. In the majority of the cases, these ratios contributed reduction in the FoS and an increment in the XDIS and SSI.

$$FoSR = \frac{FoS\ (with\ water\ table)}{FoS\ (without\ water\ table)} \tag{5.2}$$

$$XDISR = \frac{XDIS\ (with\ water\ table)}{XDIS\ (without\ water\ table)} \tag{5.3}$$

$$SSIR = \frac{SSI\ (with\ water\ table)}{SSI\ (without\ water\ table)} \tag{5.4}$$

Figure 5.8 summarizes the safety factor ratio on varying the water table for different dump slope heights from 30 to 270 m. In low dump height, no water table impact was observed. The 60 m dump height also followed the same trend, but a minor change was observed after the 70% water table height. In 90 m dump height, no deflection was observed between 10-25%, a small change was observed between 25-60%, and FoS reduced from 0.99 to 0.93 times from 60-100% water table height. The moderate range of dump height showed significant deflection, i.e., 120 to 180 m, and the intermediate influence was depicted by 210 to 270 m dump height for 40 to 100% of the water table. The maximum reduction of FoSR was found in a 180 m dump height of 20% at 100% of the water table.

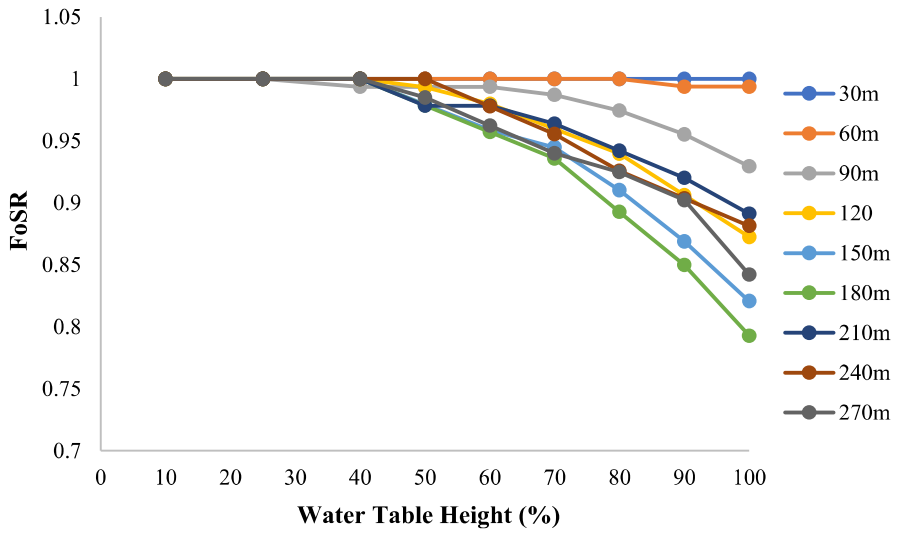

Fig. 5.8 Change in safety factor ratio with water table

Figure 5.9 (a) illustrates the change in the ratio of maximum horizontal displacement along with variation in the water table height. The XDISR curve trend reflected more sensitivity than the FoS curve. In 30 m dump height, the XDISR enhanced from 4 to 133 times compared to static condition by varying the water table from 10 to 100% of dump height and it increased nonlinearly with a very high rate. Similarly, XDISR also increased in 60 m dump height from 1.5 to 80 times for the considered range of water table height. At 90 m dump height, the XDISR was reduced by 70% at the 10% water table and merged with static state XDIS at 25%, as presented in Figure 5.9 (c). In the case of dump height from 120 to 270 m, the XDISR was dropped between 10 to 25% of the water table height, and it amplified significantly after 25%, but it was not as intense as it was for the 30 to 60 m dump height. Like the safety factor ratio, the moderate range dump height experienced more change in XDISR compared to the high dump slope structures (Figure 5.9 (b)).

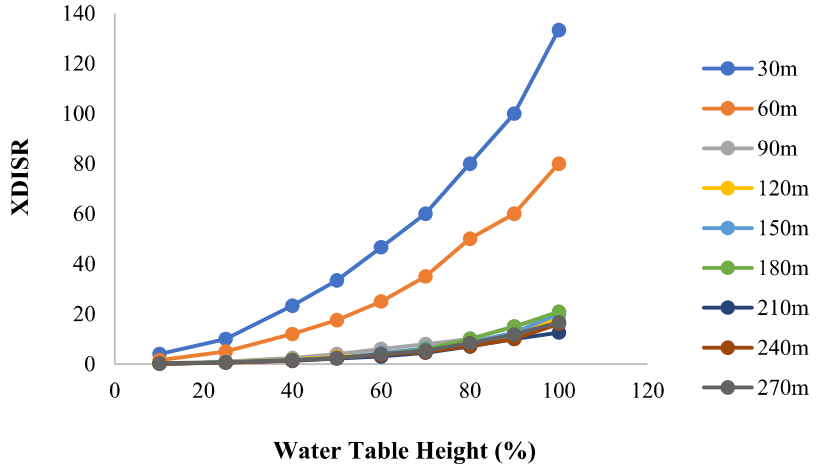

(a)

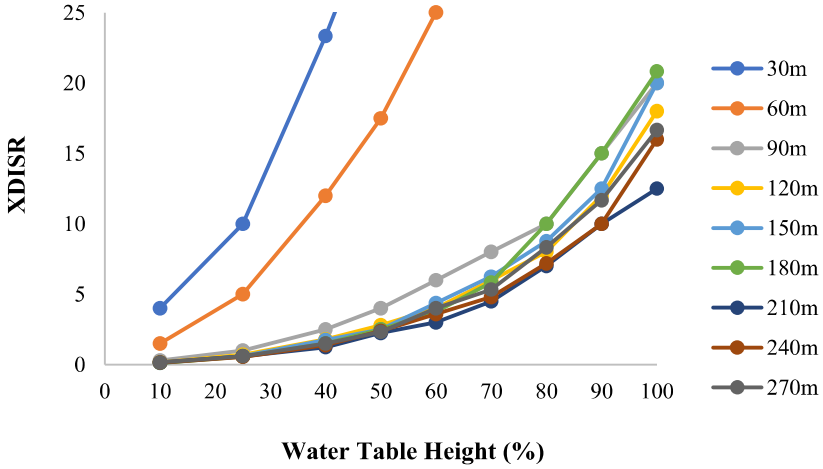

(b)

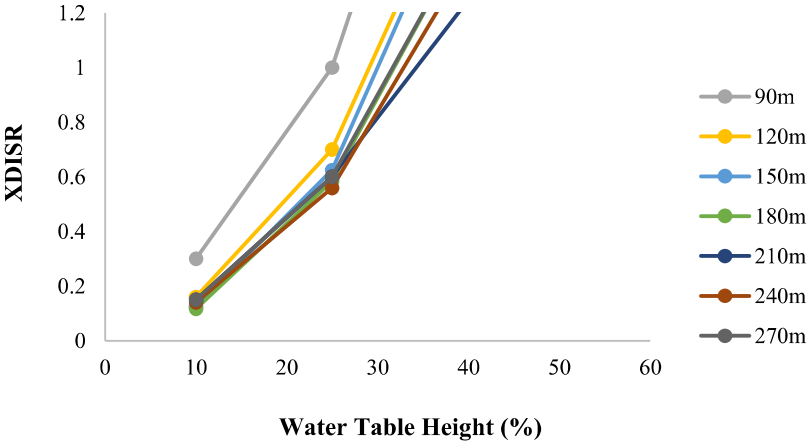

(c)

Fig. 5.9 Change in horizontal displacement ratio with water table

The shear strain increment ratio was aggravated with the increase in the water table for the adopted range of the dump height (Figure 5.10). A significant change was observed in the 30 m dump height SSIR like XDISR. It magnified from 10 to 100 times on increasing the water table from 10 to 100% (Figure 5.10 (a)). The SSIR rose 50 times on changing the water table up to 90%, and it changed drastically after 90% and covered the remaining 50% between 90 to 100%. At 60 m dump height, the SSIR reduced at 10% water table and then increased gradually up to 90% and changed drastically after 90 to 100%. The variation of the water table from 10 to 60% reduced the SSIR for the dump height between 90 to 270 m compared to the static condition, as presented in Figure 5.10 (b). The moderate range dump height from 90 to 180 m depicted a significant change in the SSIR compared to the high dump height range from 210 to 270 m. The SSIR increased after the 60% water table, but an abrupt and inconsistent nature was seen in the moderate and high range dump height.

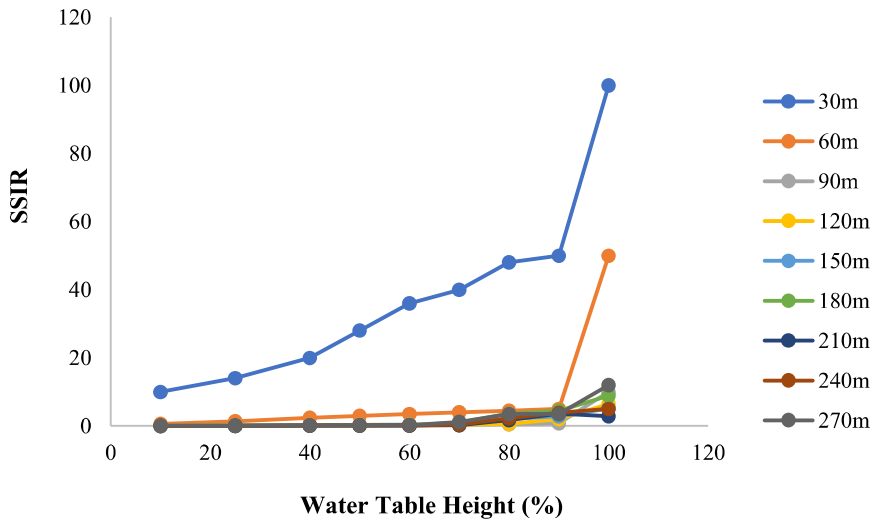

(a)

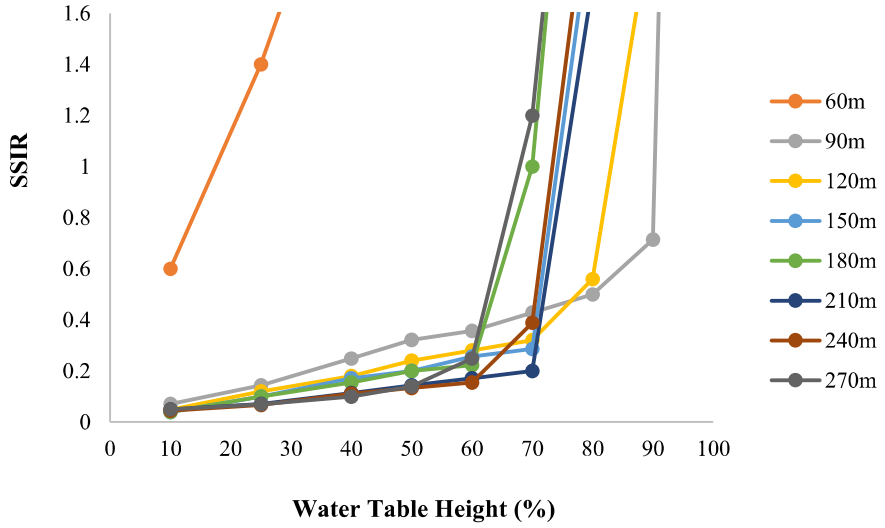

(b)

Fig. 5.10 Change in shear strain increment ratio with water table

The presence of a water table poses a significant influence on the stability of the dump slope structure. The overall effect of the water table was summarized precisely using XDIS and SSI compared to FoS. In Figures 5.9 and 5.10, it was observed that the increment ratio of XDIS and SSI was significantly higher in 30-60 m dump height when compared with 90-270 m. Therefore, the behaviour of the XDIS and SSI of the low (30 m), medium (150 m), and high (270 m) dump slope structures was analyzed at the worst condition, i.e. 100% water table height.

Figure 5.11 shows the horizontal displacement of the 30 m dump height in the static (or absence of water table) and the presence of a water table. The XDIS was negligible in the static condition, i.e. 0.015 mm (Figure 5.11 (a)). The maximum XDIS was concentrated just behind the crest area. In the presence of the water table, the XDIS increased to 2 mm, greater than 100 times the static condition displacement (Figure 5.11 (b)). The slope surface did not experience high displacement and the settlement of the OB material took place near the edge of right-hand side boundary. The SSI was also negligible in the static condition, i.e. 0.0000025 (Figure 5.12 (a)), and increased 100 times in the presence of a

water table, i.e. 0.00025 (Figure 5.12 (b)). The SSI plot also pointed to the same vulnerable zone as predicted by max XDIS.

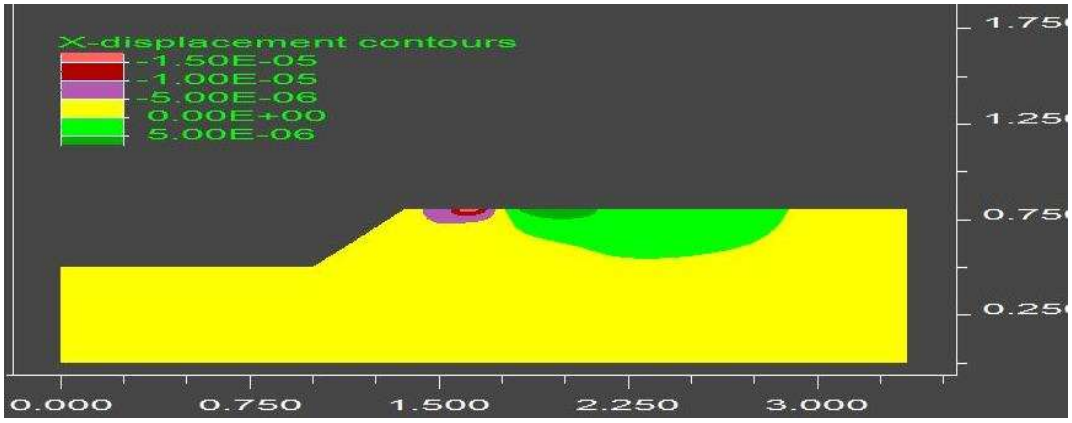

(a) Absence of water table

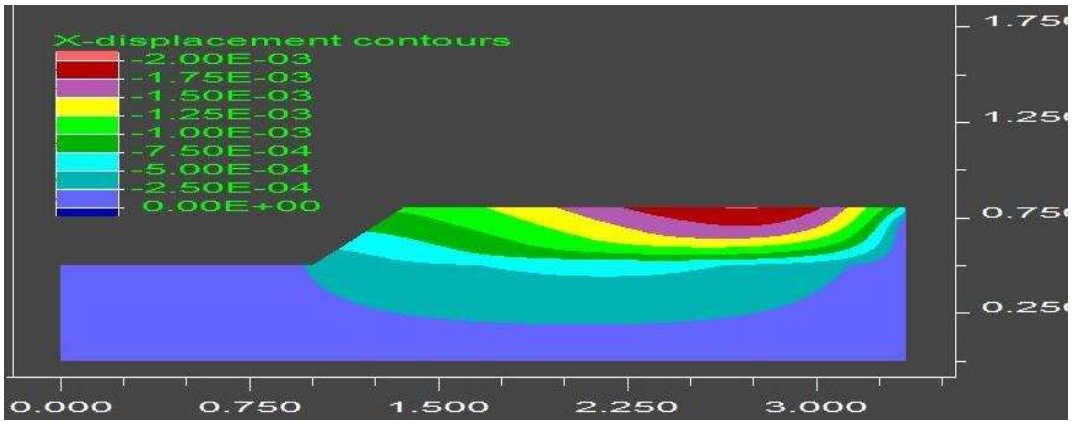

(b) Presence of water table

Fig. 5.11 Maximum horizontal displacement of 30 m dump height (1 unit of X & Y axis = 100m)

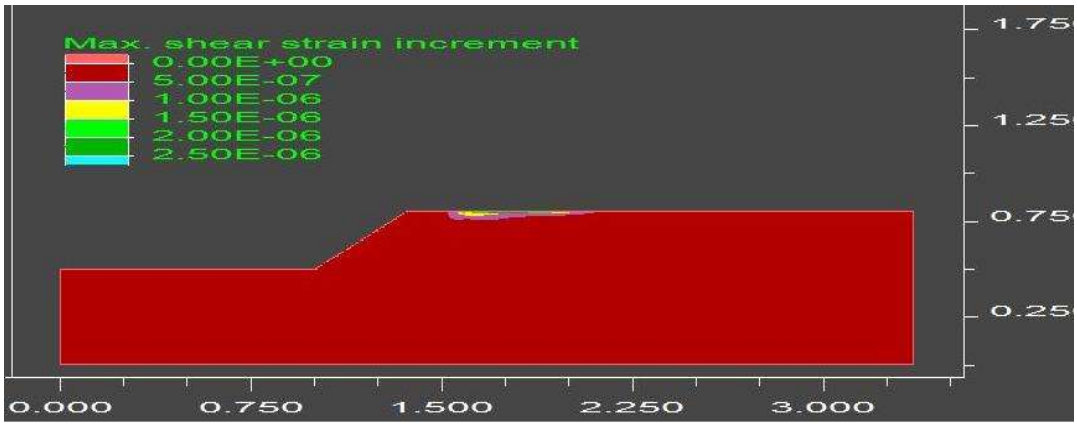

(a) Absence of water table (1 unit of X & Y axis = 100m)

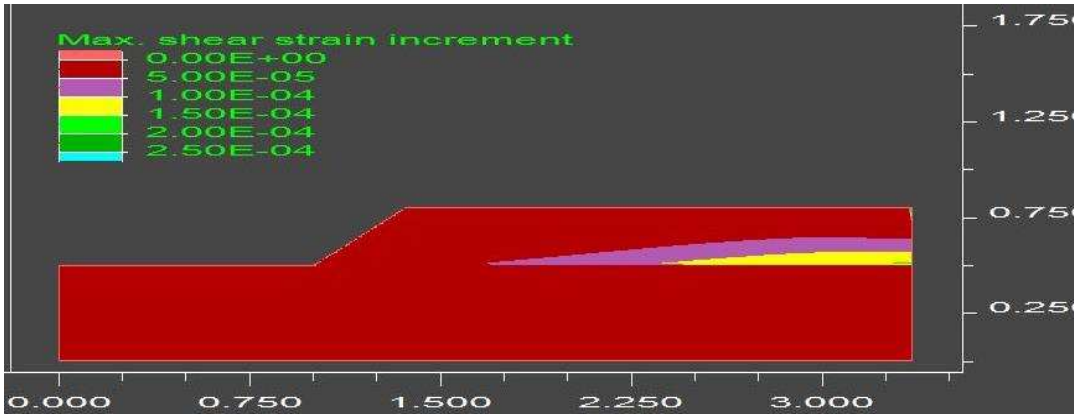

(b) Presence of water table (1 unit of X & Y axis = 100m)

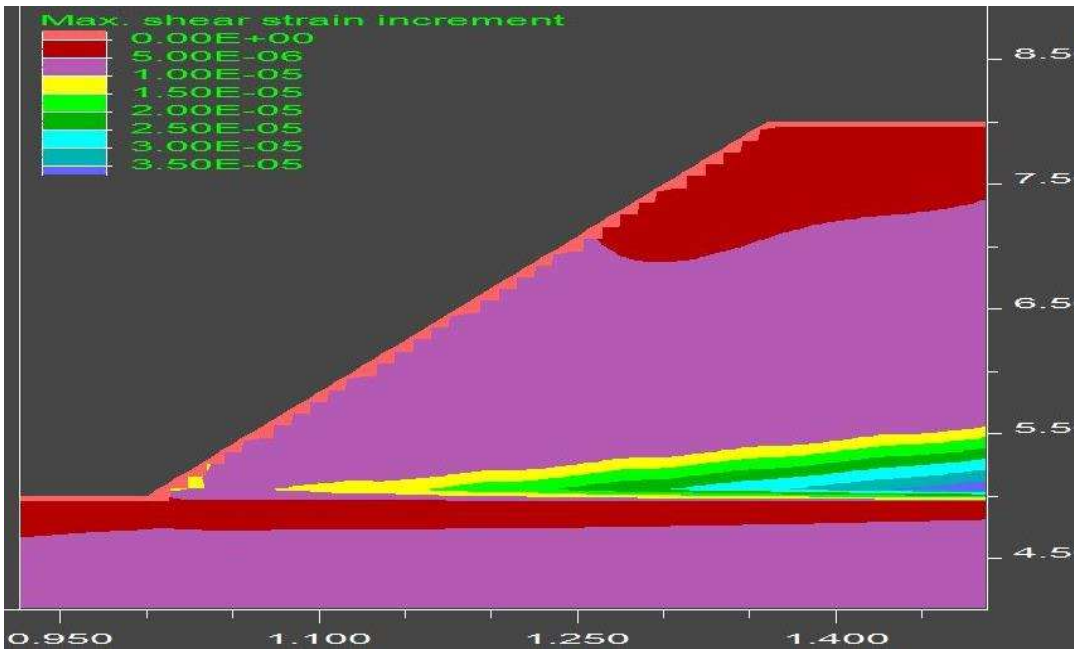

(c) Presence of water table (1 unit of X = 100m & Y axis = 10m)

Fig. 5.12 Shear strain increment of 30 m dump height

The XDIS magnified from 4 to 80 mm in 150 m dump height with the amplification of the SSI from 0.00175 to 0.009 (Figures 5.13 and 5.14) due to the presence of the water table. In the absence of the water table, the bottommost 2nd and 3rd benches experienced max XDIS (Figure 5.13 (a)). When the water table was absent, Figure 5.14 (a) shows that the max SSI was present in the toe of the bottommost 2nd and 3rd bench. In the presence of a water table, the topmost bench experienced max XDIS (Figure 5.13 (b)). All benches, except the bottommost, possessed greater than 10 mm displacement. The settlement of the OB material took place just behind the crest of the top most bench. The max SSI was also observed in the top most bench Figure 5.14 (b).

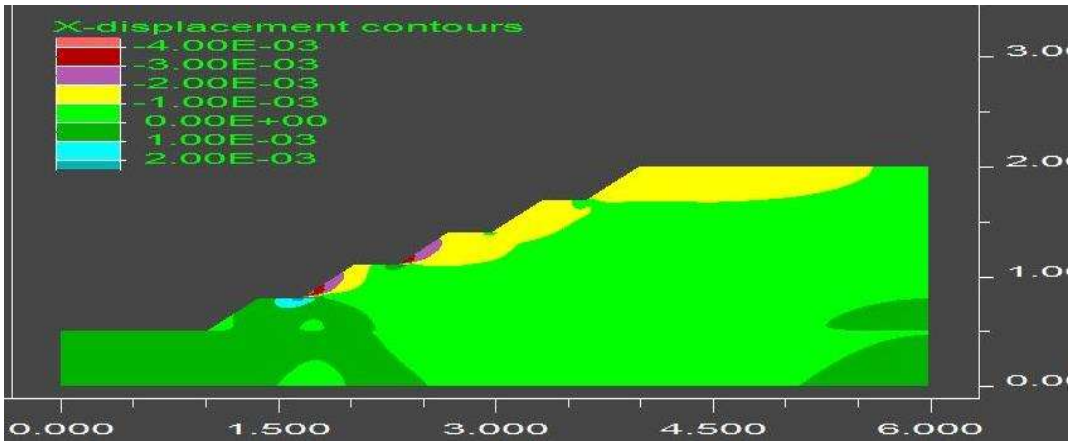

(a) Absence of water table

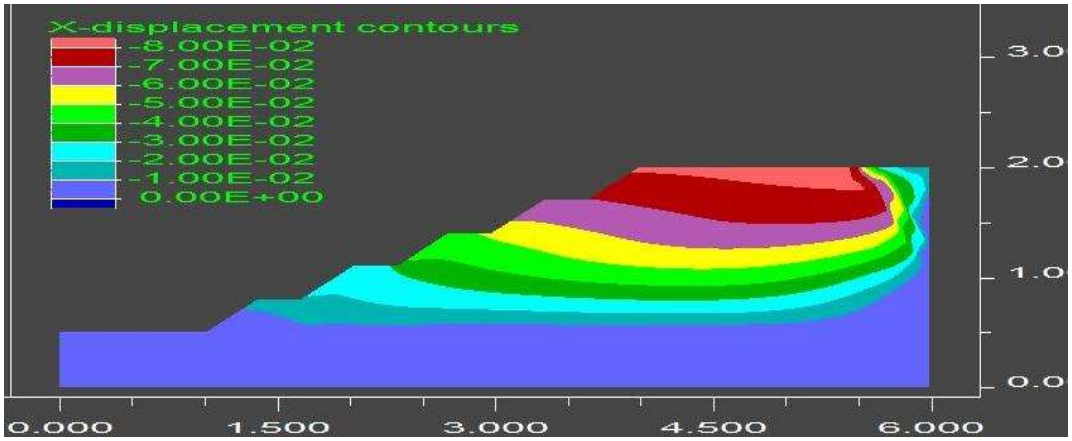

(b) Presence of water table

Fig. 5.13 Maximum horizontal displacement of 150 m dump height (1 unit of X & Y axis = 100m)

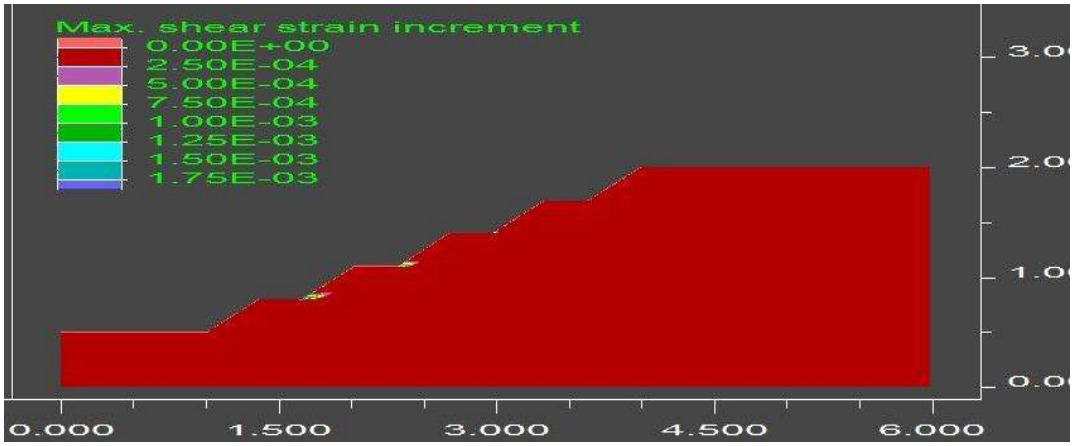

(a) Absence of water table

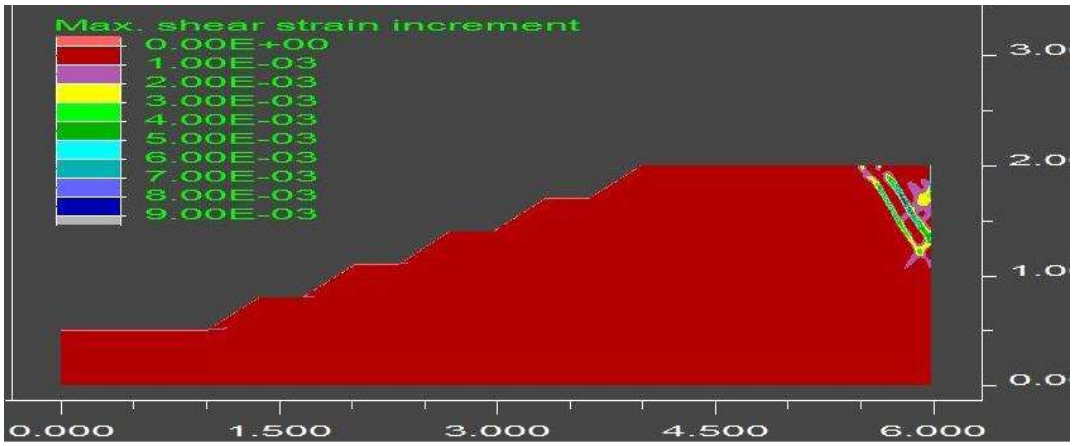

(b) Presence of water table

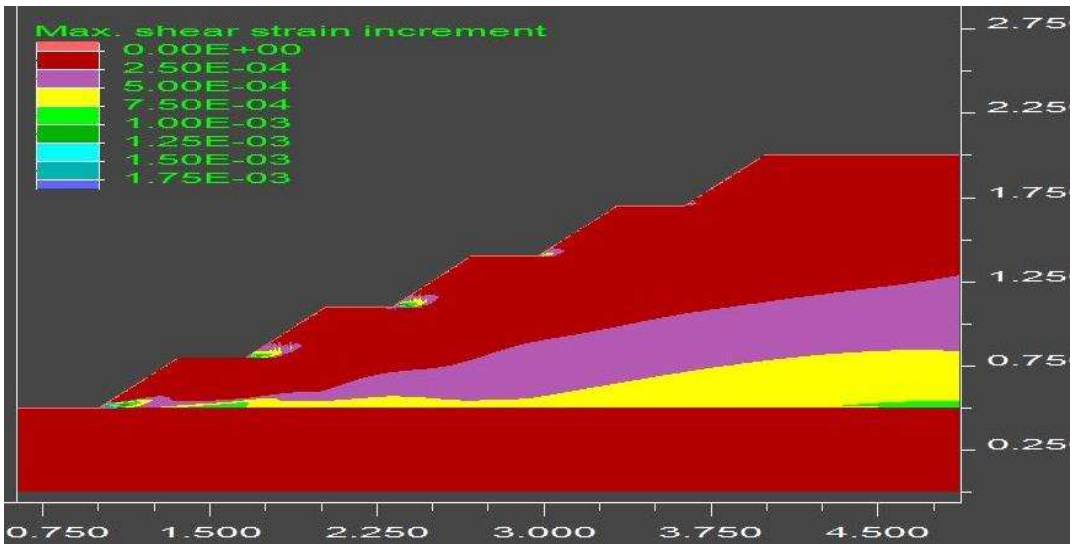

(c) Presence of water table

Fig. 5.14 Shear strain increment of 150 m dump height (1 unit of X & Y axis = 100m)

In the case of 270 m dump height, the XDIS drastically changed from 15 to 250 mm and the SSI enhanced from 0.005 to 0.06 (Figures 5.15 and 5.16) due to the water table. Figure 5.15 (a) depicts that middle benches impacted with max XDIS in the static condition and bottommost benches were less influenced. Figure 5.15 (b) illustrates that due to the presence of the water table, the topmost bench had max XDIS and it reduced towards the bottom benches. The bottom most 4 benches experienced displacement between 150 to 200 mm. In the static condition, the max SSI was present in the range of middle benches as shown in Figure 5.16 (a), and it appeared in the top bench and the toe of the bottom bench with a high extent (Figure 5.16 (b)).

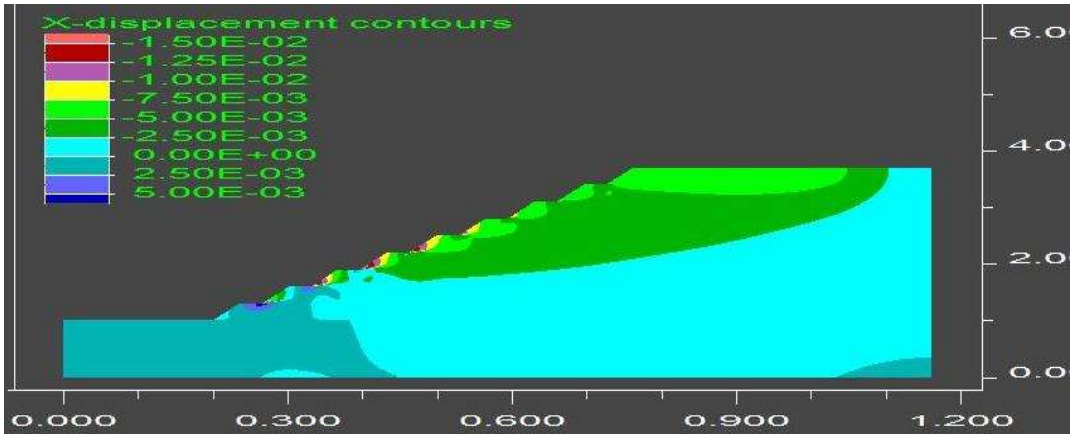

(a) Absence of water table

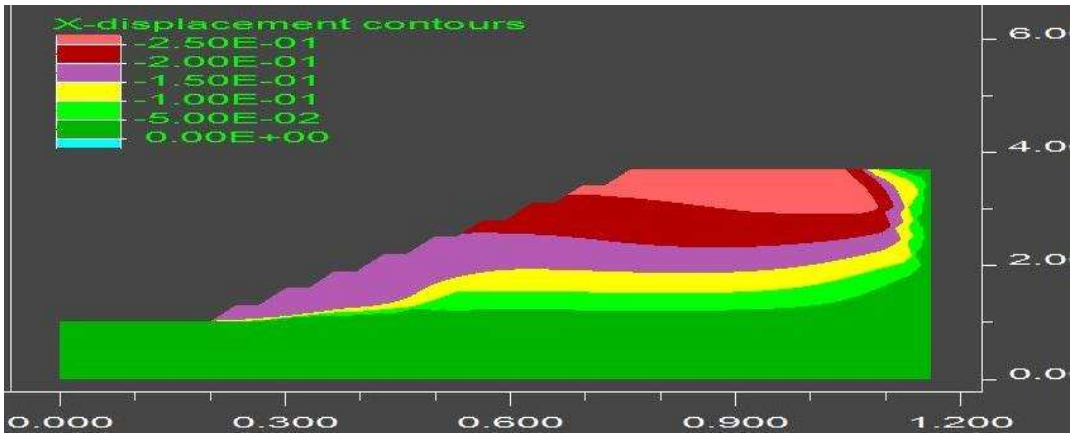

(b) Presence of water table

Fig. 5.15 Maximum horizontal displacement of 270 m dump height (1 unit of X = 1000m & Y axis = 100m)

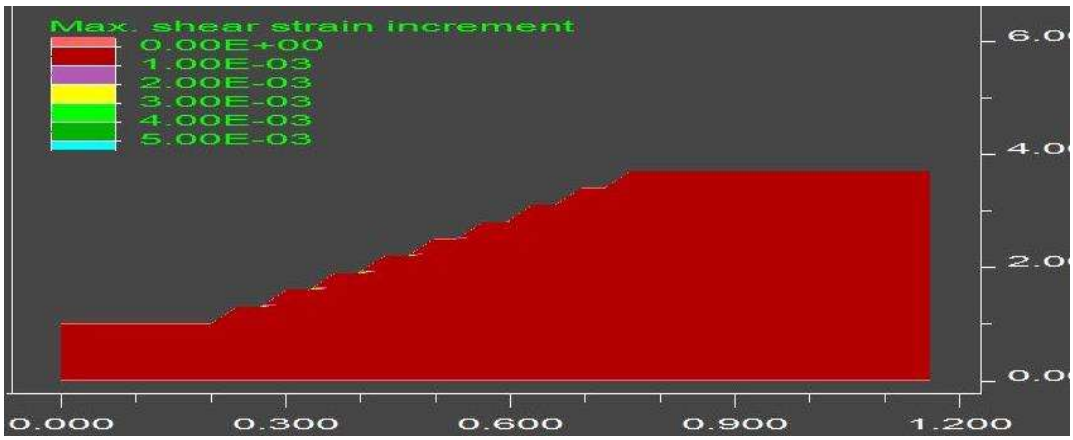

(a) Absence of water table (1 unit of X =1000m & Y axis = 100m)

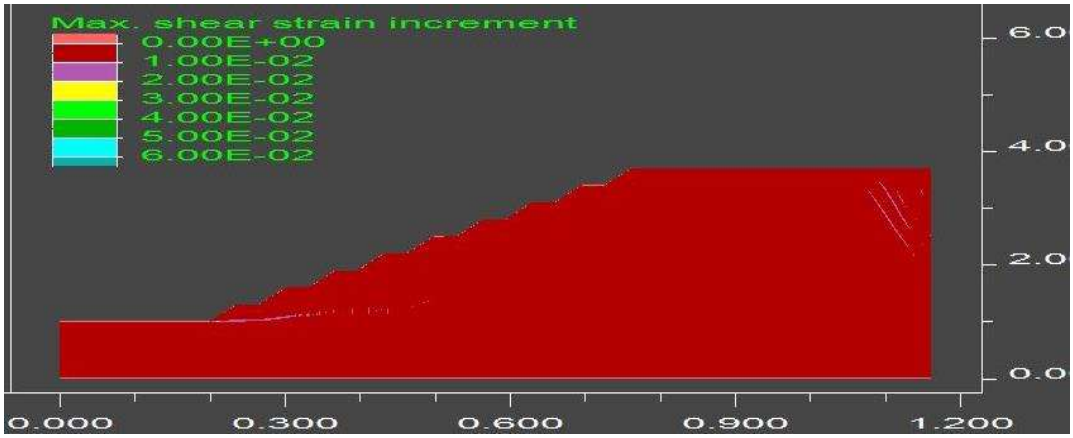

(b) Presence of water table (1 unit of X = 1000m & Y axis = 100m)

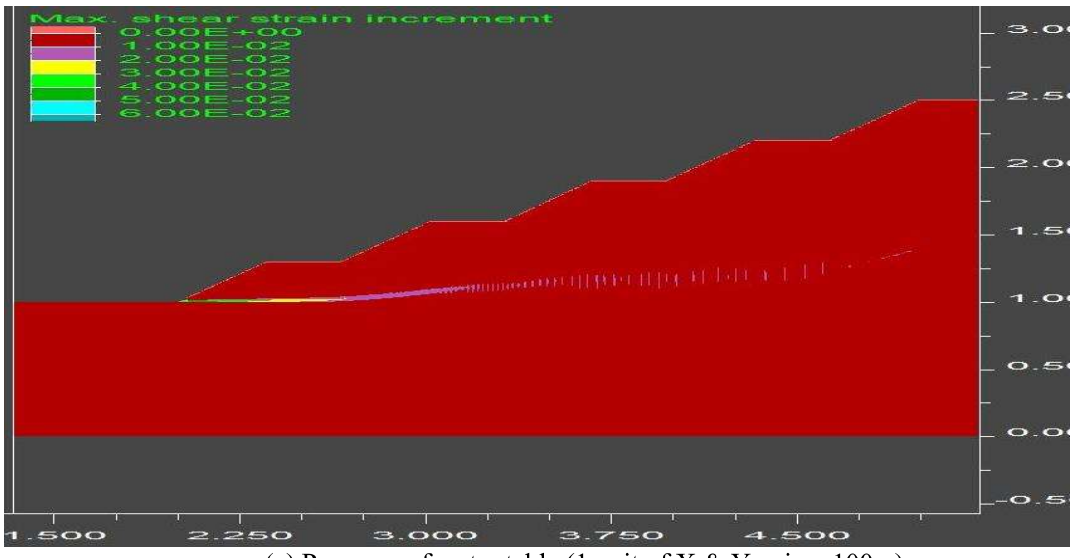

(c) Presence of water table (1 unit of X & Y axis = 100m)

Fig. 5.16 Shear strain increment of 270 m dump height

It was observed from Figures 5.11 (b), 5.13 (b), and 5.15 (b) that, in the presence of a water table, the top area of the dump slope structure experienced maximum horizontal displacement. The XDIS was reduced towards the bottom benches. The magnitude of the XDIS was observed in the form of a band. The band width increased from a low to high dump slope structure. The max XDIS influenced area moved from the right hand side edge to the crest of dump slope structures when incorporating water table from low to high dump slope structures. Figures 5.12 (c), 5.14 (c), and 5.16 (c) depict that the initiation of the slip surface started from the drainage point of the bench in low, medium, and high dump slope structures.

5.6. Summary

This chapter discussed the procedure of statistical model development and the significance of the FoS, XDIS, and SSI for the evaluation of the stability state of the dump slope structures. The stability state of the dump slope structures was classified into three states along with the range of performance assessment parameters. The response of the dump slope structure towards the water table with the change in behaviour of the FoS, XDIS, and SSI was also studied.